ACS Chemical Neuroscience

Research Article

pubs.acs.org/chemneuro

Single-Cell Metabolomics: Changes in the Metabolome of Freshly Isolated and Cultured Neurons

Peter Nemes,[†] Ann M. Knolhoff, Stanislav S. Rubakhin, and Jonathan V. Sweedler*

Department of Chemistry, University of Illinois at Urbana−Champaign, 600 South Mathews Avenue, Urbana, Illinois 61801, United States

Supporting Information

ABSTRACT: Metabolites are involved in a diverse range of intracellular processes, including a cell's response to a changing extracellular environment. Using single-cell capillary electrophoresis coupled to electrospray ionization mass spectrometry, we investigated how placing individual identified neurons in culture affects their metabolic profile. First, glycerol-based cell stabilization was evaluated using metacerebral neurons from *Aplysia californica*; the measurement error was reduced from ∼24% relative standard deviation to ∼6% for glycerol-stabilized cells compared to those isolated without glycerol stabilization. In order to determine the changes induced by culturing, 14 freshly isolated and 11 overnight-cultured neurons of two metabolically distinct cell types from *A. californica*, the B1 and B2 buccal neurons, were characterized. Of the more than 300 distinctive cell-related signals detected, 35 compounds were selected for their known biological roles and compared among each measured cell. Unsupervised multivariate and statistical analysis revealed robust metabolic differences between these two identified neuron types. We then compared the changes induced by overnight culturing; metabolite concentrations were distinct for 26 compounds in the cultured B1 cells. In contrast, culturing had less influence on the metabolic profile of the B2 neurons, with only five compounds changing significantly. As a result of these culturing-induced changes, the metabolic composition of the B1 neurons became indistinguishable from the cultured B2 cells. This observation suggests that the two cell types differentially regulate their *in vivo* or *in vitro* metabolomes in response to a changing environment.

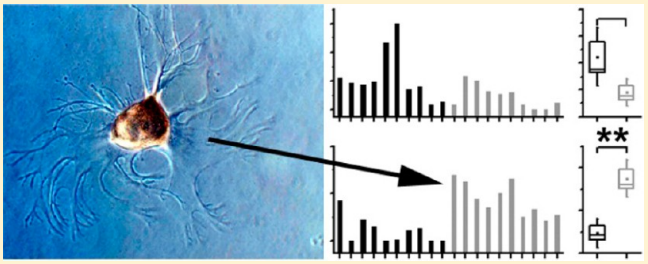

KEYWORDS: *Neuron culture, neurotransmitter, metabolome, single-cell analysis, capillary electrophoresis mass spectrometry, Aplysia californica*

Cellular heterogeneity is multifaceted and often dynamic. Depending on internal and external processes, cells with an identical genotype may develop or exhibit phenotypical differences.[1] Variations in phenotype can translate into altered cellular behaviors; for example, the existence of drug-resistant phenotypes may explain the incomplete eradication of cancer cells by pharmaceutical treatments.[2] In general, biological systems achieve a balance between stability and plasticity[3] by influencing physiological activity. For example, neuronal plasticity is implicated in learning, while stability is needed to maintain memory.[4] By characterizing the key biochemical components involved in physiological and pathological processes, we can better understand the specific mechanisms underlying cellular plasticity and stability.

The metabolome, in particular, provides the opportunity to assess the biological state of individual cells. Unlike many processes affecting the genome, transcriptome, and peptidome, metabolic pathways are readily influenced by both intrinsic and extrinsic factors, are highly dynamic, and entail diverse compound types. It is, therefore, not surprising that the metabolome has been considered as the best descriptor of the phenotype.[5] Metabolomic measurements in small sample sizes, and across a broad range of analyte amounts in individual cells, require specialized approaches in microsampling and separation, and exceptional performance in detection. Analytical advances in the development of diverse detection schemes underpinning these single-cell measurements have been the focus of recent reviews,[6−11] and so are not covered here.

Of the various analytical platforms allowing single-cell investigations, mass spectrometry (MS) provides excellent overall figures of merit, is typically label-free, attains high sensitivity and low limits of detection, and is capable of structure-specific compound identification and quantitation. In addition, MS uses a range of sampling and ion generation approaches that can be tailored for specific cell sizes, analyte types, and experimental conditions.[9,11−14] Among many examples, metabolites and peptides in individual mammalian and molluscan cells were profiled or quantified using matrix-assisted laser desorption/ionization (MALDI) MS.[15−20] Intact metabolites were detected with striking sensitivity in single cancer cells by nanostructure initiator MS,[21,22] and in unicellular algae and bacteria by high-density microarray

Received: July 16, 2012
Accepted: August 24, 2012
Published: August 25, 2012

Table 1. Statistically Significant Changes in Metabolite Abundances in Single Neurons of the *A. californica* CNS[a]

identifier	compd	MCC in ASW vs glycerol	B1 vs B2	cultured B1 vs cultured B2	freshly isolated vs cultured B1	freshly isolated vs cultured B2
1	acetylcarnitine	–	↑**	–	↑**	–
2	acetylcholine	n/a	↓**	↓*	–	↑*
3	adenosine	↓**	–	–	–	–
4	alanine	–	↑**	–	↑**	↑*
5	β-alanine	–	–	–	↑*	–
6	β-alanine betaine	–	↑**	–	↑**	–
7	GABA	–	↑*	–	↑*	–
8	arginine	↓**	↑**	–	↑*	–
9	aspartic acid	–	↑*	–	↑*	–
10	carnitine	–	↑**	–	↑**	–
11	choline	–	↑*	–	↑**	–
12	cytidine	↓**	–	–	–	–
13	glutamic acid	–	↑**	–	↑**	–
14	glutamine	↑**	↑*	–	↑*	–
15	glutathione	↑*	↑**	–	↑**	–
16	glycine	↑*	↑*	–	–	↓**
17	glycine betaine	–	↑*	–	↑*	–
18	histamine	↓**	–	n/a	–	n/a
19	histidine	–	–	–	–	↓*
20	indoleacrylic acid	–	–	–	↑*	–
21	isoleucine	–	↑**	–	↑**	–
22	leucine	–	↑**	–	↑**	–
23	lysine	–	↑**	–	↑**	–
24	nicotinamide	–	–	–	–	–
25	ornithine	↑*	–	–	–	–
26	phenylalanine	–	↑**	–	↑**	–
27	proline	↑*	↑*	–	↑*	–
28	proline betaine	–	↑**	–	↑**	–
29	serine	↑*	↑*	–	↑*	–
30	serotonin	↓*	n/a	n/a	n/a	n/a
31	thiamine	–	–	–	↑**	–
32	threonine	–	↑**	–	↑**	–
33	tryptophan	–	↑**	–	↑*	–
34	tyrosine	–	↑**	–	↑**	↓*
35	valine	–	↑**	–	↑**	–

[a]Arrows (↑ and ↓) denote relative signal changes of statistical significance (e.g., adenosine ion abundance was lower in MCC neurons isolated in ASW than in 33% glycerol). Asterisk (*) and two asterisks (**) mark *p*-values below 0.05 and 0.005, respectively, and were calculated among extracts of freshly isolated MCC_{1-4} and glycerol-stabilized MCC_{5-8} MCC cells, $B1_{1-5}$ B1 cells, $B2_{3-7}$ B2 cells, $cB1_{1-5}$ cultured B1 cells, and $cB2_{1-5}$ cultured B2 cells. Dash (–) indicates no statistically significant differences, $p > 0.05$. Not applicable, n/a, denotes insufficient signal intensity.

MS.[23] With an ∼100-nm-scale spatial resolution, secondary ion MS has been used to probe characteristic vitamin E[24] and lipid[25] distributions at the soma–neurite junction of neurons, helping to decipher lipidomic changes in the membrane of mating unicellular organisms.[26] Furthermore, ambient ion sources extended MS to experimental conditions native to many live specimens.[14] Live video MS,[27] laser ablation electrospray ionization,[28,29] and femtosecond laser desorption ionization[30] have been used to directly analyze and differentiate between states of individual plant and animal cells.

Single-cell MS often benefits from implementing separation prior to detection; separation reduces sample complexity, which in turn enhances peak capacity, detection limits, quantitation, and analyte identification. Electrophoresis in a capillary or a microfluidic channel is particularly advantageous for cellular analyses because it offers favorable scaling laws that allow miniaturization to a volume regime that is compatible with individual cell measurements.[31] As one example, single erythrocytes were injected into a microfluidic device and lysed; the hemoglobins were then separated and detected at a reasonable throughput (ca. 12 cells min^{-1}).[32] Complementing this approach, the integration of capillary electrophoresis (CE) with electrospray ionization (ESI) high-resolution time-of-flight (TOF) MS was used to measure over 100 signals in a single neuron;[33] this was made possible by adapting the technology to low sample volumes (6 nL), low detection limits (300 amol), and a wide linear dynamic range for quantitation (nM to μM concentration range). More recently, CE-ESI-MS with multivariate data processing was used to differentiate over 50 neurons from six different types, based on their respective chemistries.[34]

One of the key elements in a successful single-cell investigation is careful sample preparation. It is desirable to sample a cell without material loss so as to address potentially low analyte levels. This step can be complicated by inherent cell stability; for example, larger *Aplysia californica* neurons are mechanically more fragile than smaller ones, and cultured cells are likewise less stable than freshly isolated cells. Glycerol treatment helps to preserve cell integrity and, in some cases, cellular functions under physiological and cryogenic con-

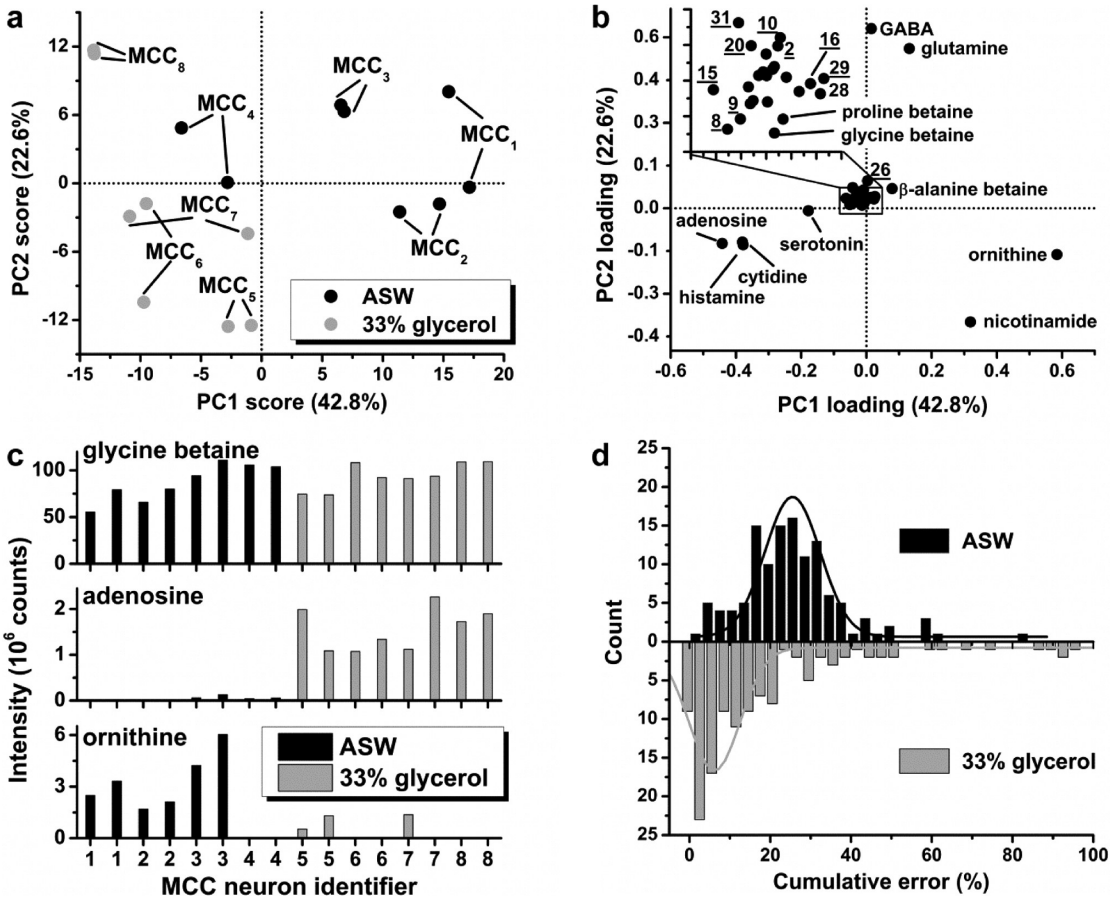

Figure 1. Analyte extraction strategies for single isolated MCC neurons of the *A. californica* CNS. (a) PCA score plot of the CE-ESI-MS data revealed differences between sample extracts: cells isolated in ASW and 33% glycerol-ASW solutions form separate data clusters. Duplicate analytical measurements are included. (b) The PCA loading plot helped to identify specific metabolic differences between the cell extracts. Underlined numbers correspond to compounds identified in Table 1. (c) The composition of the cell-isolation solution had a pronounced effect on extraction efficiency for many, but not all, metabolites. For example, when isolating neurons in glycerol-ASW, the ion signal intensities did not appreciably vary for glycine betaine, significantly increased for adenosine, and decreased for ornithine. Bars correspond to individual cells measured in technical duplicates. (d) Histograms show the cumulative measurement error as RSD for 35 metabolites measured in duplicate. Gaussian curves (solid lines) fitted on these data had a median and width of ~24% (RSD) and ~16% for cells isolated in ASW, and ~6% (RSD) and ~13% for those treated with 33% glycerol-ASW. The higher analytical reproducibility offered by glycerol stabilization was beneficial for assessing chemical changes upon neuron culturing. Key: MCC_{1-4} = freshly isolated and MCC_{5-8} = glycerol-stabilized MCC cell extracts.

ditions.[35,36] Likewise, glycerol at sufficient concentrations can improve the mechanical stability of both freshly isolated and cultured *A. californica* neurons, which in turn helps to maintain their integrity when undergoing physical manipulation for single-cell isolation.[15] However, it is not clear how this treatment may influence the underlying metabolome of cells.

Here we validate a glycerol-based cell sampling protocol using one cell type, the metacerebral cells (MCCs), by single-cell CE-ESI-MS. We next measure changes in neuronal metabolic profiles induced by culturing using morphologically and biochemically similar buccal B1 and B2 neurons[37,38] isolated from the central nervous system (CNS) of *A. californica*. These peptidergic motoneurons have a cell body of ~100−150 μm in diameter and share a biochemical microenvironment in the CNS (see Figure S1, Supporting Information); they both innervate the gut, and appear to utilize identical neuropeptides as neuromodulators.[39−41] Although B2, but not B1, cells contain acetylcholine transferase,[42] the exact nature of the biochemical differences between these identified neurons is not fully understood. Here we examine how these two similar neurons respond to their extracellular environment. Our results highlight the dynamic nature of the cellular metabolome, and demonstrate the importance of validating the sampling approaches and data evaluation associated with such individual cell experiments.

RESULTS AND DISCUSSION

Validating and Optimizing Single-Neuron Sample Preparations. To validate our protocols for cell isolation and analysis, we conducted a comparative metabolic analysis of *A. californica* MCCs isolated in artificial seawater (ASW) with those treated with 33% glycerol in ASW. Their relatively large size (~180 μm in average diameter) and defined location in the CNS make these cells readily recognizable and, therefore, an excellent model for this portion of the study. Furthermore, because MCCs have a well-defined neurochemistry, and have been extensively used for single cell investigations,[43−45] they allow comparisons of sample preparation protocols in relationship to prior studies.

Two sets of MCC neurons, each containing four cells, were isolated in ASW (MCC_{1-4}) or in a glycerol-containing solution (MCC_{5-8}). Neurons were swiftly rinsed with ~1 μL of

dx.doi.org/10.1021/cn300100u | ACS Chem. Neurosci. 2012, 3, 782−792

deionized water in order to minimize the presence of inorganic salts and compounds in the extracellular environment, then placed into an acidified methanol solution to extract endogenous compounds. The neuron extracts, and some of the rinse solutions, were analyzed with a single-cell CE-ESI-MS platform.[33] Over 300 cell-related, distinct ion signals (m/z values) were detected in the MCC extracts. Adapting our previously established approach,[34] 35 of these ion signals were ascribed to metabolites encompassing classical neurotransmitters and amino acids (Table 1). These compounds, and their corresponding ion signal abundances, were treated as a net representation of intracellular neuron chemistry and as a collective history of the sample preparation and analytical measurements. To gauge the technical aspects, chemical profiles were extracted for the identified ions and analyzed.

Unsupervised principal component analysis (PCA) was implemented to identify chemical patterns among the extracts, permitting us to compare and validate two protocols used for cell isolation, followed by chemical analysis. CE-ESI-MS peak areas corresponding to the selected metabolites (see Methods) were transformed into a combination of orthogonal principal components (PCs) and loading values (see Figure 1). The first five PCs, in order of significance, accounted for 42.8% (PC1), 22.6% (PC2), 15.5%, 6%, and 4.5% of the variance in the data. Explaining over ∼65% of the cumulative variance, PC1 and PC2 were sufficient for further chemometric data analysis. The corresponding score plot (Figure 1a) shows neuron content measurements acquired in duplicate. Some variations were apparent between the technical replicates (e.g., see data pairs for MCC_1 and MCC_7), and are in line with the prior reported technical errors in analysis using this measurement system.[34] Most data points corresponding to the MCC cells isolated in ASW clustered distinctively from those prepared in 33% glycerol. Thus, the score plot underscores the systematic chemical differences between the extracts obtained using both neuron isolation protocols, and demonstrates that these protocols are not mutually interchangeable.

PCA conjoined with statistical analysis of the data was implemented to discern if there were differences in analyte abundances between the two types of extracts. The PCA loading plot (Figure 1b) reported the contribution of each compound in the net variation calculated in the score plot. The majority of analyte data points clustered near the origin, indicating insignificant variations in abundances, despite differences in the sample preparation protocols. Student's t tests further confirmed that the mass spectrometric signals corresponding to these ions did not exhibit statistically significant differences among the two protocols (see Table 1). As an example, the glycine betaine signal areas were comparable among all extracts (Figure 1c).

In contrast, other metabolites formed data clusters in distinct quadrants of the loading plot, confirming systematic biases in extraction yields; for example, adenosine, histamine, cytidine, and serotonin populated the lower left quadrant in Figure 1b. The signal intensity for adenosine neared the detection limit in the ASW-based cell extracts, whereas it had a high signal-to-noise ratio in the glycerol-treated extracts (Figure 1c). These differences in analyte concentration were of statistical significance (Table 1). In contrast, ornithine was measured in a consistently higher concentration in the ASW-isolated neurons (Figure 1c). Not surprisingly, the ornithine and nicotinamide data points are located in a different quadrant of the loading plot (see lower right region), revealing chemical biases of a different kind during sample preparation. Statistical data analysis confirmed that these biases in extraction were of significance (Table 1). Likewise, glutamine and γ-aminobutyric acid (GABA) separated in the topmost region of the plot, indicating biased extraction, albeit with lower analytical repeatability (data not shown).

The notion of systematic biases between the two protocols was partially corroborated by analyzing the rinse solutions collected during neuron isolation. Analyte levels were determined in the chemical environments of the representative MCC_1 neuron isolated in ASW and MCC_6 neuron harvested in 33% glycerol. The rinse solution of the former did not contain ornithine in a detectable amount but contained adenosine in high abundance. In contrast, the MCC_6 rinse solution was abundant in ornithine, whereas adenosine reached an order of magnitude lower ion signal level. Although these effects were confirmed to be statistically significant, we speculate that a common cause underlies the chemical biases observed between the cell isolation protocols; however, the origin of the detected systematic biases is not clear.

Considering that MCC neurons are serotonergic, and that the glycerol-treated MCC extracts contained significantly higher levels of serotonin, it is possible that cell isolation in the glycerol-based environment reduced the stimulated release of this neurotransmitter, or perhaps its accidental leakage. A similar reasoning could account for the consistent biases noted for the adenosine, cytidine, and histamine measurements. The opposite observations for ornithine and nicotinamide levels may be explained via the removal of extracellular compounds during rinsing or enhanced compound release in the glycerol-containing environment. Clearly, additional experiments (e.g., via selective probes) can help to evaluate these scenarios.

Adequate technical repeatability is a prerequisite for comparative studies, in this case, assessing whether culturing influences the cell metabolome. Thus, we further characterized measurement repeatability by comparing MCC cell extracts obtained under ASW with those under glycerol-treated conditions. The cumulative error in the ion signal intensities for 35 metabolites was determined for two analytical replicates from four different neurons under each isolation protocol. The results are presented as histograms in Figure 1d. Normal distributions fitted on the data yielded a median value of ∼24% and ∼6% relative standard deviation (RSD) for the ASW- and glycerol-based protocols, respectively. Gaussian widths of the distributions were comparable. These results suggest that a high concentration of glycerol was beneficial for the metabolic analysis of single neurons, complementing observations in prior peptidomic studies.[15,17] Glycerol treatment appeared to help cells withstand physical handling and removal of external matrix, and/or minimized the active release of intracellular compounds, aiding the metabolic analysis as a result.

It is interesting to note that the higher analytical repeatability when using the glycerol treatment corroborated reported data on cell morphology. Past[15] and present microscopic investigations have shown that *A. californica* cells isolated in ASW are relatively fragile, and are typically lysed upon contact with air or prolonged exposure to distilled water. In contrast, glycerol-treated neurons demonstrate a good stability, allowing single cells to be exposed to air or even divided into aliquots for follow-up studies. However, the time frame of the glycerol treatment is noted to impose constraints on cell stability. Exposure to glycerol for up to several minutes stabilized the entire cell, whereas prolonged contact seemed to cause cell

dx.doi.org/10.1021/cn300100u | ACS Chem. Neurosci. 2012, 3, 782−792

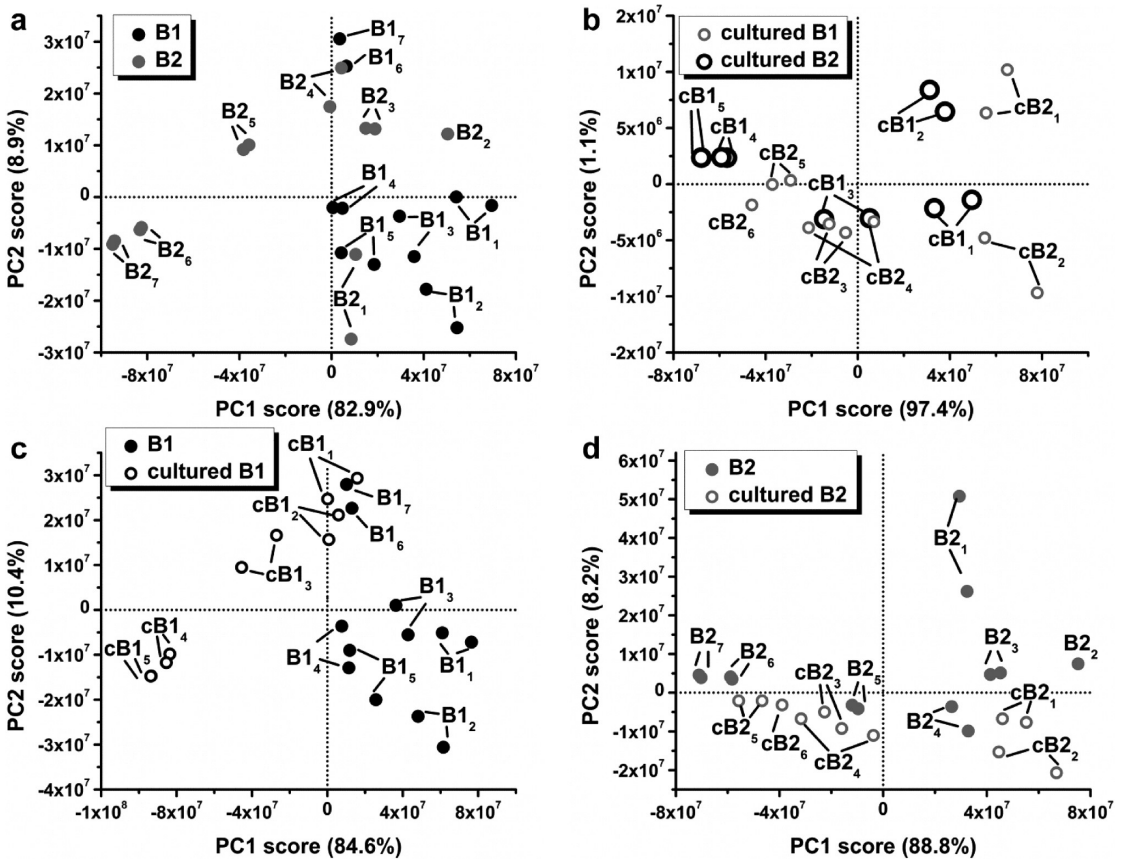

Figure 2. Metabolic differentiation between freshly isolated and cultured neurons of *A. californica*. (a) PCA score plots of the CE-ESI-MS data uncovered differences in metabolite abundances between the freshly isolated B1 and B2 neurons. (b) In contrast, these neurons possessed indistinguishable chemistries after cell culture. Respective loading plots are shown in Figure S2. Metabolic differences were (c) clear between the freshly isolated and cultured B1 cells and (d) minor between the freshly isolated and cultured B2 neurons. These results indicate that despite metabolic dissimilarities in the freshly isolated state, B1 and B2 neuron chemistries became similar upon culturing. Key: $B1_{1-7}$ = freshly isolated B1; $B2_{1-7}$ = freshly isolated B2; $cB1_{1-5}$ = cultured B1; and $cB2_{1-6}$ = cultured B2 neuron extracts. Technical replicate measurements are included.

membranes to become more plastic and transparent (results not shown). Nonetheless, appropriate glycerol treatment facilitated cell collection and rinsing of inorganic salts, without apparent visible damage to the cells. With improvements in measurement repeatability, and no detectable systematic biases deducible by examination of the chemical data and comparing it to known data on these cells, glycerol treatment was used for the second portion of the study, investigating metabolic changes in cultured neurons.

Metabolic Differences among Freshly Isolated Neurons. The relationship between chemistry and neuron identity was probed for one pair of similar neurons in the *A. californica* CNS, the peptidergic motoneurons B1 and B2 of the buccal ganglion. More specifically, a systematic series of experiments were designed to study the relationship between the metabolic content of B1 and B2 neurons and the extracellular environment. These buccal neurons in the *A. californica* CNS present themselves as two symmetrical pairs. Single neurons dissected from one ganglion were placed individually in culture dishes and cultured overnight in ASW supplemented with antibiotics. Neurons of the contralateral pair served as a control; the freshly isolated B1 and B2 neurons were extracted soon after isolation. A total of seven B1 ($B1_{1-7}$) and seven B2 freshly isolated neurons ($B2_{1-7}$) were prepared, as were five cultured B1 ($cB1_{1-5}$) and six cultured B2 neurons ($cB2_{1-6}$). The neurons were isolated in 33% glycerol prepared with ASW, then quickly rinsed with deionized water, and placed in acidified methanol solution to extract intracellular analytes. Neuron extracts were measured using the single-cell CE-ESI-MS platform and methodology described above (see also Methods). By ensuring similar initial conditions for the neurons in this portion of the study (freshly isolated cells used for all experiments), as well as consistency in chemical analysis, this experimental design permitted the detection and interpretation of cell culturing-related changes in the metabolomes.

To determine the respective neuronal chemical profiles, 35 identified compounds (Table 1) were measured in the resulting extracts in technical duplicates. Unsupervised PCA indicated appreciable chemical differences between many, but not all, of the freshly isolated B1 and B2 extracts (Figure 2a). The first three PCs, in order of decreasing significance, accounted for 82.9% (PC1), 8.9% (PC2), and 4.8% of the variance in the data. Explaining greater than ~90% of the variance, further analysis was limited to the PC1 and PC2 components. The calculated score plot is presented in Figure 2a and the loading plot is shown in Figure S2a in the Supporting Information. The score plot revealed that extracts of most of the freshly isolated B1 neurons (see $B1_{1-5}$) separated from those of the freshly isolated B2 cells (see $B2_{2-7}$). Separation was less striking for the extracts of freshly isolated $B1_6$ and $B1_7$ cells, and diminished for $B2_1$. The results on the MCC neurons established that the implemented protocols in manual neuron isolation and

dx.doi.org/10.1021/cn300100u | *ACS Chem. Neurosci.* 2012, 3, 782–792

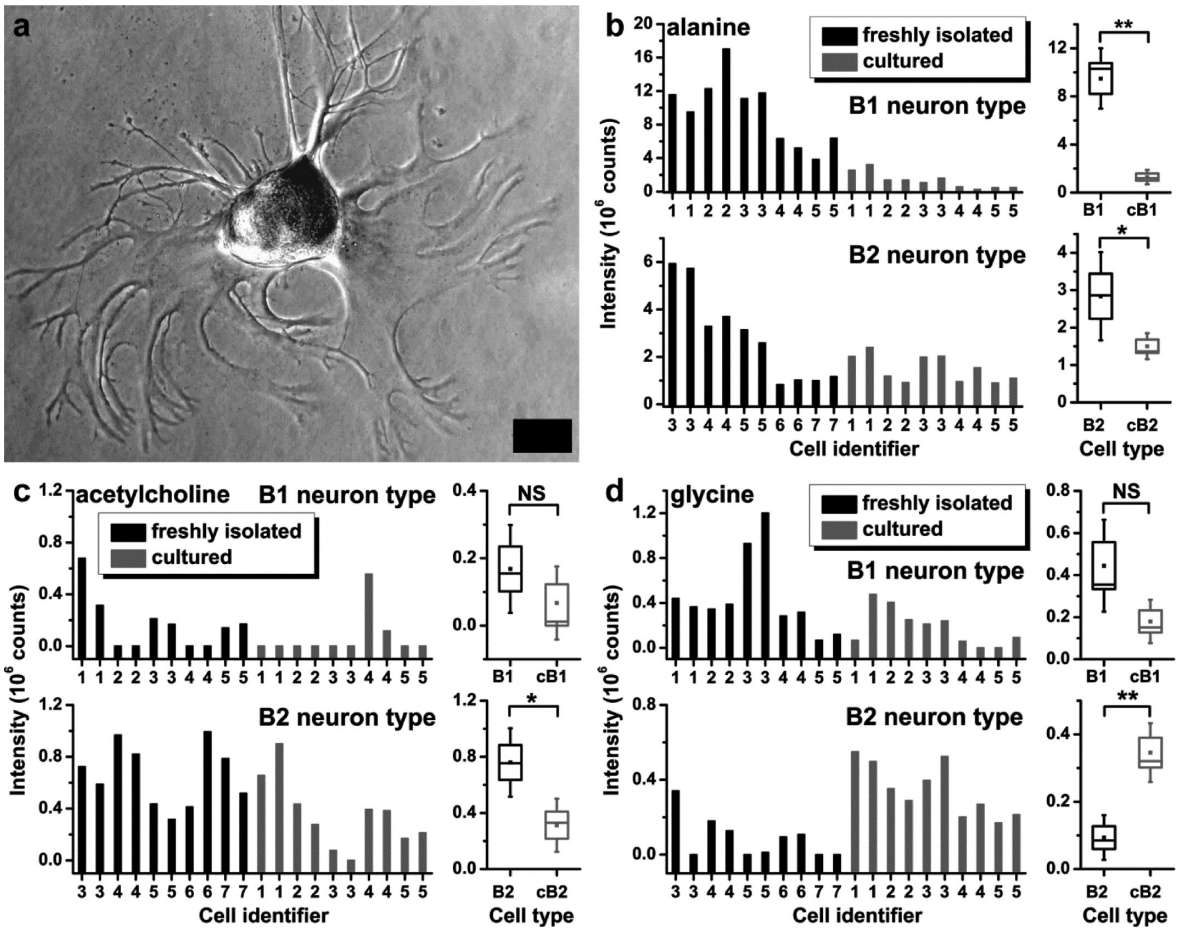

Figure 3. Morphological and statistically significant metabolic changes upon single-cell culturing. (a) In culture, B1 and B2 neurons typically formed a network of neurites overnight, as demonstrated in the microscope image of a representative cultured B2 cell. (b) Statistical analysis of the data revealed that culturing imposed cell-type dependent variations in neuron chemistries. For example, both neuron types in culture became depleted in alanine. (c) Acetylcholine abundance decreased in the B2 but not the B1 neurons. (d) In stark contrast, other compounds such as glycine accumulated in the B2 neurons only. Bars correspond to individual cells measured in technical duplicates. Key: square, box, and whisker represent statistical median, standard error, and confidence interval, respectively. NS labels statistically insignificant variations, and asterisk (*) and two asterisks (**) mark *p*-values below 0.05 and 0.005, respectively. Scale = 50 μm.

instrumental measurement ensured good measurement repeatability, therefore, the noted neurons likely corresponded to biological variation. Nonetheless, the majority of B1 and B2 neurons showed cell type-dependent metabolic composition.

The disparities between the B1 and B2 neuron chemistries rose to statistical significance. Statistically appreciable differences in ion signal abundance were observed for a large number of compounds (Table 1) between the B1 neurons, $B1_{1-5}$, and B2 neurons, $B2_{3-7}$; the $B1_6$, $B1_7$, and $B2_1$ neurons were excluded based on statistical analysis of the data (data not shown). The majority of the identified metabolites yielded higher ion signal responses in the B1 extracts. Representative examples included energy carriers (e.g., carnitine and acetylcarnitine), amino acids (e.g., alanine and arginine), osmolites (e.g., β-alanine betaine and proline betaine), and an antioxidant (e.g., glutathione). Although B1 neurons have not been reported to express acetylcholine transferase, a few of the B1 extracts tested here contained acetylcholine in minimal amounts. In contrast, the B2 extracts consistently yielded acetylcholine with 8−10-fold higher ion signal intensities than those registered in the B1 extracts. Statistical analysis confirmed that the B2 neuron extracts contained a higher abundance of acetylcholine (see Table 1). In line with this observation, B2 neurons have been noted to convert choline into acetylcholine.[42]

These analytical results reveal a metabolic dissimilarity between most of the B1 and B2 neurons, which is somewhat surprising given the biological similarities reported in the literature.[39−42] Notably, the present findings highlight subtle differences between these cell types that went unnoticed in our previous large-scale metabolic profiling work that involved over 140 distinct ions. In light of the prominent chemical differences found among the other tested neurons (MCC, R2, R15, and left pleural (Pl1) neurons), the B1 and B2 data points essentially overlapped during PCA (see Figure 3 in ref 34). The current protocols in sample preparation, measurement, and data analysis targeted to 35 different metabolites conferred higher technical reproducibility (~6% error vs ~24% RSD), and demonstrated an ability to appreciate the fine differences between the B1 and B2 metabolite profiles. These technical and methodological improvements in detection and data interpretation are crucial in assessing subtle metabolic changes.

Metabolic Changes in Cultured Neurons. A metabolic comparison of freshly isolated and cultured neurons revealed that culturing induced metabolic alterations in the B1 and B2 neurons. Figure 2 presents pairwise PCA score plots calculated

dx.doi.org/10.1021/cn300100u | ACS Chem. Neurosci. 2012, 3, 782−792

utilizing the CE-ESI-MS data. The respective loading plots are provided in Figure S2. The score plots reveal that cell culturing modified the metabolic profiles of the neurons. A drastic change in chemistry is apparent when comparing the differences between the freshly isolated (Figure 2a) and cultured cells (Figure 2b). As shown in Figure 2c, most B1 neurons ($B1_{1-5}$) are located in opposing regions of the score plot than their cultured counterparts ($cB1_{1-5}$), indicating noticeable metabolic changes for the cultured cells. Of the variances in the mass spectrometric data, the first three PCs, in order of significance, described 84.6% (PC1), 10.4% (PC2), and 2.5% between the freshly isolated and cultured B1; 88.8% (PC1), 8.2% (PC2), and 1.6% between the freshly isolated and cultured B2; and 97.4% (PC1), 1.1% (PC2), and 0.9% between the cultured B1 and B2 neurons. Further analyses were limited to PC1 and PC2 components since they accounted for more than ∼95% of the variance. In parallel, marginal separation is noted in Figure 2d between the freshly isolated ($B2_{2-7}$) and cultured B2 neurons ($cB2_{1-6}$); relative to the B1 neurons, it appears that culturing caused a minimal metabolic shift in the B2 neurons. Furthermore, cultured B1 and cultured B2 neurons formed overlapping data points in the score plot (Figure 2b), suggesting that the underlying chemistries became comparably variable.

Modulations in the metabolite abundances were confirmed to be statistically significant. As inferred from the loading plots (see Figure S2), culturing impacted the amounts of certain analytes (e.g., osmolites and small acids) in the cells. Student's *t* test was implemented to further statistically evaluate the noted changes (Table 1). The calculated graphs between the freshly isolated and cultured neuron extracts are presented for the B1 neurons in Figure S3 and the B2 cells in Figure S4. A pairwise comparison of the data confirmed that despite the significant chemical dissimilarities in their freshly isolated chemical composition, the B1 and B2 neurons became similar in metabolic profile after culturing; only acetylcholine was present in a different amount with a higher concentration in the cultured B2 neurons. The transition of two metabolically distinct cell types becoming indistinguishable as a result of culturing was studied further by attending to the variations of specific compounds.

Culturing affected analyte amounts in a distinct manner in each of the neuron types. Figure 3 shows that more extensive changes in composition accompanied the culturing of the B1 compared to the B2 cells. The cultured B1 neurons were depleted in most of the monitored small molecules, whereas several showed insignificant variances in abundance. As an example, cultured neurons of both cell types contained significantly lower amounts of alanine (Figure 3b) and similar levels of adenosine, cytidine, and ornithine (Figures S2 and S3). A closer statistical inspection noted that shifts in analyte concentrations were dependent on neuron type. Certain compounds were more abundant in the freshly isolated B1, but not the freshly isolated B2 neurons (e.g., see acetylcarnitine, GABA, and proline betaine in Table 1). This trend reversed for acetylcholine; freshly isolated neurons of the B2, but not the B1 type, contained the compound in higher amounts (Figure 3c). Concurrently, culturing caused other compounds (e.g., histidine and glycine) to accumulate in the B2 cells but not B1 (Figure 3d). A combined trend was noticed for tyrosine, which was depleted in the B1 neurons and increased in the B2 cells upon culturing. These outcomes confirm that culturing led to complex chemical changes in the studied neurons.

Clearly, our results demonstrate that the two morphologically and positionally similar neurons respond differently to cell culture. The data also suggest that the extracellular environment influenced the metabolome to a higher extent in the B1 neurons compared to the B2. Others have suggested similar results in other systems; culturing in a serum-free medium has been reported to induce lipidomic changes in lymphocytes, which are capable of reversing diet-induced shifts in fatty acid composition.[46] Here, some of the culturing-induced changes in the B1 and B2 metabolic profiles may also be linked to potentiation of cell-to-cell signaling mechanisms that act to reconnect neurons. For example, glycine, an NMDA receptor modulator, facilitates neuron outgrowth in the spinal cord of mice.[47] Higher glycine concentrations were measured in the B2 neurons. However, the altered glycine levels in the cultured B1 neurons were not statistically significant enough to support this explanation.

Prior studies on various model organisms aid in the interpretation of the observed metabolic alterations. For example, extracellular glutamate triggers spine formation and shapes early neural connectivity in mice.[48] In *A. californica*, the lower glutamic acid observed in the cultured B1 neurons may indicate active release of the compound in order to guide the formation of neuron connections. However, glutamic acid concentration did not appreciably change in the B2 neurons during culturing. GABA, another coordinator of neuronal networks, is a modulator of neuronal proliferation and migration, and inhibits neurite formation in rats.[49−51] Furthermore, it is released from the axonal growth cones of hypothalamic neurons in mice.[52] The lower GABA concentrations seen in the cultured B1 neurons seem to be in accord with extensive outgrowth formation (Figure 3a). However, variation in the GABA amounts was not of statistical significance in the B2 neurons, and so this does not support a similar connection. Furthermore, culturing is also known to modulate the expression of amino acid-transporter mRNAs in microvascular endothelial cells.[53] It follows, therefore, that the changes in amino acid levels may in part be due to cell-specific mechanisms balancing release and reuptake of these molecules. Simultaneous measurement of other -omic approaches, such as transcriptomics and proteomics, can help to obtain corroborative evidence.

■ CONCLUSIONS

It is intriguing to speculate on the link between the chemical changes observed here and neuronal plasticity. Our findings revealed that the metabolomes were significantly altered in the B1 neurons in culture, but not the B2, and demonstrated the ability of CE-ESI-MS to uncover metabolic changes in neurons upon culturing. More importantly, our results underscore the dynamic nature of cellular heterogeneity. As is apparent for the B1 and B2 buccal neurons of *A. californica*, extrinsic factors, including microenvironments, significantly influence the metabolic heterogeneity of single cells. In spite of the dissimilar metabolic profiles exhibited by the *in vivo*/freshly isolated B1/B2 neurons, their respective metabolic chemistries underwent significant changes in response to culturing. Furthermore, not only did adaptation to solitary and nutrient-deficient microenvironments influence their cell chemistry, it also resulted in the disparate metabolite profiles of the B1 and B2 cultured neurons becoming similar. By combining this empirical readout of cellular metabolite profiles with proteomic, transcriptomic, and genomic data, we can further probe the mechanistic details

of variations in cell-to-cell heterogeneity to answer remaining questions. For example, we are curious as to whether the changes between these two neuron types are related to chemical plasticity under isolated culturing conditions (of a single neuron alone), or whether they are due to their sparse cellular and nutrient-deficient environment.

Follow-up experiments may be helpful in determining the reasons for the differences we observed in the responses of these neurons. For example, adjusting the composition of the culturing media (e.g., by adding nutrients), or including additional neurons or other supporting cells in close physical proximity, may result in similar or different outcomes. By implementing appropriate coculturing techniques, and ensuring that suitable compounds are present in the media, we may be able to maintain chemical features of cultured neurons that are comparable to freshly isolated cells; or these neurons may exhibit differences, such as distinct neurite development and chemical connections between cells. Alternatively, nutrients or other cells may be added postculturing in ASW in an effort to restore cellular metabolites to freshly isolated conditions.

Future biological studies aside, measurement enhancements will aid follow-up studies. After all, although the analytical workflow described is effective at measuring hundreds of cell-related signals in various individual neurons, these sampling and metabolic measurement approaches require expertise in sample isolation, sample preparation, instrumentation operation, and have moderate throughput. Clearly, improvements in technology, methodology, and data interpretation would allow more comprehensive studies. Ideally, single-cell experiments should involve a large number of cells in order to obtain representative data, and to also account for the diversity of the dynamic interactions that cells encounter in a community. A number of advances can be adapted to CE-ESI-MS, aiding us in achieving these goals. As examples, the chemical microenvironments around cells can be precisely controlled by specialized microsources,[54,55] the success rate of cell sampling can be increased via cytometry and micromolded magnetic rafts,[56] and isolated cells can be analyzed with decreasing analysis times and increasing dimensionality, using advances in microfluidics and separation schemes.[32,57]

As a final point, our data underscores the importance of experimental design in metabolomics measurements. Culturing causes significant but distinct changes in the B1 and B2 neuron chemistries, which in turn may affect their responses to biological as well as environmental cues. As cell cultures *in vitro* have been widely used in experimentation, and are emerging for high-impact applications spanning from routine toxicological screenings[58] to formulating artificial organs,[59] it is essential to validate cultured cells (and lineages) against freshly isolated cells. The techniques and methodologies discussed here present options for the comparison of metabolic states among selected cells, and so should also create an opportunity to follow modulation of cellular functional states.

METHODS

Chemicals. Methanol was purchased from Fisher Scientific (Fair Lawn, NJ) and formic acid from Thermo Scientific (Rockford, IL). All other chemicals were obtained at gradient grade or higher from Sigma-Aldrich Co. (St. Louis, MO) and used as received. Sample extracts were kept in polymerase chain reaction vials purchased from MidSci (St. Louis, MO).

Animals and Single-Cell Isolation. Adult *A. californica* (175−250 g) were obtained from the National Resource for *Aplysia* (Rosenstiel School of Marine & Atmospheric Science, University of Miami, FL) between May 1 and June 1, 2010, and were maintained in continuously circulated, aerated ASW cooled to 14 °C. Animals were anesthetized by injecting 390 mM of $MgCl_2$ into the vascular cavity, equal by mass to approximately one-third of each animal's body weight. Ganglia and adjacent nerves were surgically dissected, enzymatically treated to remove connective tissues, and identified neurons were manually isolated with sharp tungsten needles (World Precision Instruments, Inc., Sarasota, FL) in ASW that consisted of 460 mM NaCl, 10 mM KCl, 10 mM $CaCl_2$, 22 mM $MgCl_2$, 26 mM $MgSO_4$, and 10 mM 4-(2-hydroxyethyl)-1-piperazineethanesulfonic acid (HEPES), at pH 7.8. Alternatively, cell isolation took place in a solution containing 33% glycerol and 67% ASW (v/v) to stabilize the cells. In order to reduce bias in sample preparation, individual experiments involved isolating symmetrical neurons from a single animal in the same day in a randomized fashion. Isolated MCC, B1, and B2 cells were rinsed with ∼1 μL of deionized water for ∼1−5 s to minimize inorganic salts and extracellular metabolites on their surfaces. Following protocols demonstrated previously,[33,34] neurons were placed into 5 μL of 50% (v/v) methanol solution prepared with 0.5% (v/v) acetic acid to facilitate analyte extraction and quench enzymatic processes *ex vivo*. Neurons were stored in the solution at −20 °C until analysis (but no longer than 3 weeks), with no noticeable degradation in extract chemistry (data not shown). The resulting extracts were centrifuged for 1 min at 2000*g* and the aliquots directly analyzed by a custom-designed single-cell analysis CE-ESI-MS system.[33] Samples were measured in a randomized manner across several days to prevent bias due to manual sample loading by the CE platform and/or potential day-to-day variability in the performance of the ESI-MS instrument.

Neuron Culturing. Identified B1 and B2 neurons were isolated in ASW and placed individually into plastic Petri tissue culture dishes (Falcon 353001, Becton Dickinson Labware, NJ). Following an earlier protocol,[60] the cells were cultured overnight at room temperature (20−25 °C) in ASW supplemented with antibiotics: 100 units/mL penicillin G, 100 μg/mL streptomycin, and 100 μg/mL gentamicin, at pH 7.8. The success of the cell culturing was determined by observing cell shape, color, translucency, and neurite outgrowth under an inverted microscope (Axiovert 25, Carl Zeiss Microscopy LLC, Thornwood, NY) (see Figure 3a). Five B1 and six B2 neurons were cultured successfully according to this protocol. The cultured cells were sampled from the Petri dish surface after replacing the culturing solution with the 33% glycerol ASW solution for 1−4 min and then removing the solution. Afterward, cells were isolated from the dish surface using a tungsten needle. Cells were washed swiftly with deionized water and subjected to analyte extraction as described above.

Single-Cell CE-ESI-MS. Each cell extract was analyzed in duplicate using a single-cell CE-ESI-MS platform.[33] The instrumental platform, operational protocol, and analytical methodology were adapted from our prior work.[34] Briefly, a volume of 6 nL from each neuron extract was hydrostatically introduced into a fused silica capillary (90 cm length, 75 μm i.d., 363 μm o.d., Polymicro Technologies, Phoenix, AZ), and a potential difference of 20 kV was applied across the capillary ends to separate the analytes over 50 min. The outlet of the separation capillary was coaxially fed into a sheath-flow electrospray ion source that does not require a nebulizer gas. A solution of 50% methanol containing 0.1% formic acid was supplied through this ion source at a rate of 750 nL/min and electrosprayed in the cone-jet spraying mode for the most efficient ion generation in the microflow regime.[61] The separation capillary outlet end was carefully positioned ∼50−100 μm into the Taylor cone for stable ion generation.

The produced ions were analyzed by a micrOTOF ESI-TOF mass spectrometer or a maXis ESI-Qq-TOF tandem MS (MS/MS) instrument (Bruker Daltonics, Billerica, MA) with 5 ppm mass accuracy and ∼8000 fwhm (full width at half-maximum) resolution at a 2 Hz spectral acquisition rate. Mass spectra were internally calibrated with sodium formate clusters that formed in the electrospray source as sodium salts eluted during the CE separation. These noncovalent clusters have been shown to offer fundamental and practical benefits for instrument mass calibration.[62] Mass calibrations utilized an enhanced quadratic equation and were performed using DataAnalysis

(version 4.0, Bruker Daltonics). MS/MS experiments with 20−35 eV collision energies facilitated molecular identifications.

Chemometric and Statistical Data Analysis. Chemometric and statistical methods were used to help in interpreting the metabolic patterns observed among the neuron extracts. Mass-to-charge (m/z)-selected ion electropherograms were generated by a 5 mDa window for 35 identified metabolites (see Table 1) and smoothed using a three-point Gaussian function. Peak areas were manually integrated in DataAnalysis and analyzed by unsupervised PCA using Markerview 1.1 (Applied Biosystems, Carlsbad, CA). Data preprocessing weighting was logarithmic or omitted, and scaling was mean center. Data were plotted in a scientific visualization software package (Origin 8.0, OriginLab Corp., Northampton, MA). Independent Student's t tests using a two-tailed distribution with equal sample variance were calculated in a statistical software package (Statistica 8.0, Statsoft, Inc., Tulsa, OK), after confirming applicability of this model on the collected data.

Safety Considerations. High voltage connections were shielded and electrically conductive parts were grounded to protect from exposure. The CE system was surrounded by a Plexiglas enclosure and featured a safety interlock-enabled door. Standard laboratory safety guidelines were followed when handling samples and solvents.

■ ASSOCIATED CONTENT

Supporting Information

Microscopy image of B1, B2, and MCC neurons in the *A. californica* CNS; PCA loading plots calculated between freshly isolated B1 and B2 neurons, cultured B1 and cultured B2 neurons, freshly isolated B1 and cultured B1 neurons, and freshly isolated B2 and cultured B2 neurons; Statistical data analysis between freshly isolated and cultured neurons of the B1 and B2 types. This material is available free of charge via the Internet at http://pubs.acs.org.

■ AUTHOR INFORMATION

Corresponding Author

*Telephone: 217-244-7359. Fax: 217-265-6290. E-mail: jsweedle@illinois.edu.

Present Address

†U.S. Food and Drug Administration, 10903 New Hampshire Ave., Building 64, Room 3068, Silver Spring, MD 20993, United States.

Author Contributions

J.V.S., P.N., A.M.K., and S.S.R. designed the research; S.S.R. collected the neurons; P.N. performed the metabolomics measurements; P.N. and A.M.K. analyzed the data; P.N. and J.V.S. interpreted the data; P.N. and J.V.S. wrote the manuscript.

Funding

The project described was supported by National Institute on Drug Abuse under Award No. P30 DA018310, the National Institute of Neurological Disorders and Stroke (NINDS) under Award No. R01 NS031609, and the National Science Foundation under Award No. CHE-11-11705. The content of this article is solely the responsibility of the authors and does not necessarily represent the official views of the award agencies.

Notes

The mention of commercial products, their sources, or their use in connection with material reported herein is not to be construed as either an actual or implied endorsement of such products by the Department of Health and Human Services. The authors declare no competing financial interest.

■ ACKNOWLEDGMENTS

The authors thank Xiying Wang for the single-neuron preparation work, Stephanie Baker for assistance in the preparation of this publication, and the UIUC School of Chemical Sciences machine shop for providing various components for the construction of the CE ESI system.

■ ABBREVIATIONS

ASW, artificial seawater; CE, capillary electrophoresis; CNS, central nervous system; cB1, cultured B1; cB2, cultured B2; ESI, electrospray ionization; MS, mass spectrometry; MCC, metacerebral cell; PCA, principal component analysis; PC, principal component; RSD, relative standard deviation

■ REFERENCES

(1) Snijder, B., and Pelkmans, L. (2011) Origins of regulated cell-to-cell variability. *Nat. Rev. Mol. Cell Biol. 12*, 119−125.

(2) Niepel, M., Spencer, S. L., and Sorger, P. K. (2009) Non-genetic cell-to-cell variability and the consequences for pharmacology. *Curr. Opin. Chem. Biol. 13*, 556−561.

(3) Turrigiano, G. G., and Nelson, S. B. (2004) Homeostatic plasticity in the developing nervous system. *Nat. Rev. Neurosci. 5*, 97−107.

(4) Silva, A. J. (2003) Molecular and cellular cognitive studies of the role of synaptic plasticity in memory. *J. Neurobiol. 54*, 224−237.

(5) Blow, N. (2008) Metabolomics: Biochemistry's New Look. *Nature 455*, 697−700.

(6) Borland, L. M., Kottegoda, S., Phillips, K. S., and Allbritton, N. L. (2008) Chemical analysis of single cells. *Annu. Rev. Anal. Chem. 1*, 191−227.

(7) Amantonico, A., Urban, P. L., and Zenobi, R. (2010) Analytical techniques for single-cell metabolomics: state of the art and trends. *Anal. Bioanal. Chem. 398*, 2493−2504.

(8) Salehi-Reyhani, A., Kaplinsky, J., Burgin, E., Novakova, M., Demello, A. J., Templer, R. H., Parker, P., Neil, M. A. A., Ces, O., French, P., Willison, K. R., and Klug, D. (2011) A first step towards practical single cell proteomics: a microfluidic antibody capture chip with TIRF detection. *Lab Chip 11*, 1256−1261.

(9) Lin, Y. Q., Trouillon, R., Safina, G., and Ewing, A. G. (2011) Chemical analysis of single cells. *Anal. Chem. 83*, 4369−4392.

(10) Cecala, C., and Sweedler, J. V. (2012) Sampling techniques for single-cell electrophoresis. *Analyst 137*, 2922−2929.

(11) Rubakhin, S. S., Romanova, E., Nemes, P., and Sweedler, J. V. (2011) Profiling metabolites and peptides in single cells. *Nat. Methods 8*, S20−S29.

(12) Heinemann, M., and Zenobi, R. (2011) Single cell metabolomics. *Curr. Opin. Biotechnol. 22*, 26−31.

(13) Svatos, A. (2011) Single-cell metabolomics comes of age: new developments in mass spectrometry profiling and imaging. *Anal. Chem. 83*, 5037−5044.

(14) Nemes, P., and Vertes, A. (2012) Ambient mass spectrometry for *in vivo* local analysis and *in situ* molecular tissue imaging. *Trends Anal. Chem. 34*, 22−34.

(15) Rubakhin, S. S., Greenough, W. T., and Sweedler, J. V. (2003) Spatial profiling with MALDI MS: distribution of neuropeptides within single neurons. *Anal. Chem. 75*, 5374−5380.

(16) Neupert, S., Johard, H. A. D., Nassel, D. R., and Predel, R. (2007) Single-cell peptidomics of *Drosophila melanogaster* neurons identified by Gal4-driven fluorescence. *Anal. Chem. 79*, 3690−3694.

(17) Rubakhin, S. S., and Sweedler, J. V. (2008) Quantitative measurements of cell-cell signaling peptides with single-cell MALDI MS. *Anal. Chem. 80*, 7128−7136.

(18) Zimmerman, T. A., Rubakhin, S. S., and Sweedler, J. V. (2011) MALDI mass spectrometry imaging of neuronal cell cultures. *J. Am. Soc. Mass Spectrom. 22*, 828−836.

(19) Amantonico, A., Urban, P. L., Fagerer, S. R., Balabin, R. M., and Zenobi, R. (2010) Single-cell MALDI-MS as an analytical tool for

studying intrapopulation metabolic heterogeneity of unicellular organisms. *Anal. Chem. 82*, 7394−7400.
(20) Fan, Y., Rubakhin, S. S., and Sweedler, J. V. (2011) Collection of peptides released from single neurons with particle-embedded monolithic capillaries followed by detection with matrix-assisted laser desorption/ionization mass spectrometry. *Anal. Chem. 83*, 9557−9563.
(21) Northen, T. R., Yanes, O., Northen, M. T., Marrinucci, D., Uritboonthai, W., Apon, J., Golledge, S. L., Nordstrom, A., and Siuzdak, G. (2007) Clathrate nanostructures for mass spectrometry. *Nature 449*, 1033−U1033.
(22) Greving, M. P., Patti, G. J., and Siuzdak, G. (2011) Nanostructure-initiator mass spectrometry metabolite analysis and imaging. *Anal. Chem. 83*, 2−7.
(23) Urban, P. L., Jefimovs, K., Amantonico, A., Fagerer, S. R., Schmid, T., Madler, S., Puigmarti-Luis, J., Goedecke, N., and Zenobi, R. (2010) High-density micro-arrays for mass spectrometry. *Lab Chip 10*, 3206−3209.
(24) Monroe, E. B., Jurchen, J. C., Lee, J., Rubakhin, S. S., and Sweedler, J. V. (2005) Vitamin E imaging and localization in the neuronal membrane. *J. Am. Chem. Soc. 127*, 12152−12153.
(25) Yang, H. J., Ishizaki, I., Sanada, N., Zaima, N., Sugiura, Y., Yao, I., Ikegami, K., and Setou, M. (2010) Detection of characteristic distributions of phospholipid head groups and fatty acids on neurite surface by time-of-flight secondary ion mass spectrometry. *Med. Mol. Morphol. 43*, 158−164.
(26) Kurczy, M. E., Piehowski, P. D., Van Bell, C. T., Heien, M. L., Winograd, N., and Ewing, A. G. (2010) Mass spectrometry imaging of mating Tetrahymena show that changes in cell morphology regulate lipid domain formation. *Proc. Natl. Acad. Sci. U.S.A. 107*, 2751−2756.
(27) Tsuyama, N., Mizuno, H., and Masujima, T. (2011) Mass spectrometry for cellular and tissue analyses in a very small region. *Anal. Sci. 27*, 163−170.
(28) Nemes, P., and Vertes, A. (2007) Laser ablation electrospray ionization for atmospheric pressure, in vivo, and imaging mass spectrometry. *Anal. Chem. 79*, 8098−8106.
(29) Shrestha, B., Patt, J. M., and Vertes, A. (2011) In situ cell-by-cell imaging and analysis of small cell populations by mass spectrometry. *Anal. Chem. 83*, 2947−2955.
(30) Coello, Y., Jones, A. D., Gunaratne, T. C., and Dantus, M. (2010) Atmospheric-pressure femtosecond laser imaging mass spectrometry. *Anal. Chem. 82*, 2753−2758.
(31) Lapainis, T., and Sweedler, J. V. (2008) Contributions of capillary electrophoresis to neuroscience. *J. Chromatogr. 1184*, 144−158.
(32) Mellors, J. S., Jorabchi, K., Smith, L. M., and Ramsey, J. M. (2010) Integrated microfluidic device for automated single cell analysis using electrophoretic separation and electrospray ionization mass spectrometry. *Anal. Chem. 82*, 967−973.
(33) Lapainis, T., Rubakhin, S. S., and Sweedler, J. V. (2009) Capillary electrophoresis with electrospray ionization mass spectrometric detection for single-cell metabolomics. *Anal. Chem. 81*, 5858−5864.
(34) Nemes, P., Knolhoff, A. M., Rubakhin, S. S., and Sweedler, J. V. (2011) Metabolic differentiation of neuronal phenotypes by single-cell capillary electrophoresis-electrospray ionization-mass spectrometry. *Anal. Chem. 83*, 6810−6817.
(35) Miyamoto, M. D. (1975) Binomial analysis of quantal transmitter release at glycerol treated frog neuromuscular junctions. *J. Physiol. (London, U.K.) 250*, 121−142.
(36) Pegg, D. E. (1976) Long-term preservation of cells and tissues. *J. Clin. Pathol. 29*, 271−285.
(37) Kreiner, T., Sossin, W., and Scheller, R. H. (1986) Localization of *Aplysia* neurosecretory peptides to multiple populations of dense core vesicles. *J. Cell Biol. 102*, 769−782.
(38) Lloyd, P. E., Schacher, S., Kupfermann, I., and Weiss, K. R. (1986) Release of neuropeptides during intracellular stimulation of single identified *Aplysia* neurons in culture. *Proc. Natl. Acad. Sci. U.S.A. 83*, 9794−9798.
(39) Church, P. J., Cohen, K. P., Scott, M. L., and Kirk, M. D. (1991) Peptidergic motoneurons in the buccal ganglia of *Aplysia californica*: Immunochemical, morphological, and physiological characterizations. *J. Comp. Physiol. A-Sens. Neural Behav. Physiol. 168*, 323−336.
(40) Santama, N., Brierley, M., Burke, J. F., and Benjamin, P. R. (1994) Neural network-controlling feeding in *Lymnaea stagnalis*: Immunocytochemical localization of myomodulin, small cardioactive peptide, buccalin, and FMRFamide-related peptides. *J. Comp. Neurol. 342*, 352−365.
(41) Scott, M. L., Govind, C. K., and Kirk, M. D. (1991) Neuromuscular organization of the buccal system in *Aplysia californica*. *J. Comp. Neurol. 312*, 207−222.
(42) Lloyd, P. E., Mahon, A. C., Kupfermann, I., Cohen, J. L., Scheller, R. H., and Weiss, K. R. (1985) Biochemical and immunocytological locatization of the molluscan small cardioactive peptides in the nervous system of *Aplysia californica*. *J. Neurosci. 5*, 1851−1861.
(43) Fuller, R. R., Moroz, L. L., Gillette, R., and Sweedler, J. V. (1998) Single neuron analysis by capillary electrophoresis with fluorescence spectroscopy. *Neuron 20*, 173−181.
(44) Hatcher, N. G., Zhang, X., Stuart, J. N., Moroz, L. L., Sweedler, J. V., and Gillette, R. (2008) 5-HT and 5-HT-SO4, but not tryptophan or 5-HIAA levels in single feeding neurons track animal hunger state. *J. Neurochem. 104*, 1358−1363.
(45) Stuart, J. N., Zhang, X., Jakubowski, J. A., Romanova, E. V., and Sweedler, J. V. (2003) Serotonin catabolism depends upon location of release: characterization of sulfated and gamma-glutamylated serotonin metabolites in *Aplysia californica*. *J. Neurochem. 84*, 1358−1366.
(46) Yaqoob, P., Newsholme, E. A., and Calder, P. C. (1995) Influence of cell-culture conditions on diet-induced changes in lymphocyte fatty-acid composition. *Biochim. Biophys. Acta, Lipids Lipid Metab. 1255*, 333−340.
(47) Tapia, J. C., Mentis, G. Z., Navarrete, R., Nualart, F., Figueroa, E., Sanchez, A., and Aguayo, L. G. (2001) Early expression of glycine and GABA(A) receptors in developing spinal cord neurons. Effects on neurite outgrowth. *Neuroscience 108*, 493−506.
(48) Kwon, H. B., and Sabatini, B. L. (2011) Glutamate induces de novo growth of functional spines in developing cortex. *Nature 474*, 100−104.
(49) Maric, D., Liu, Q. Y., Maric, I., Chaudry, S., Chang, Y. H., Smith, S. V., Sieghart, W., Fritschy, J. M., and Barker, J. L. (2001) GABA expression dominates neuronal lineage progression in the embryonic rat neocortex and facilitates neurite outgrowth via GABA(A) autoreceptor/Cl- channels. *J. Neurosci. 21*, 2343−2360.
(50) Gaiarsa, J. L., Kuczewski, N., and Porcher, C. (2011) Contribution of metabotropic GABA(B) receptors to neuronal network construction. *Pharmacol. Ther. 132*, 170−179.
(51) Sernagor, E., Chabrol, F., Bony, G., and Cancedda, L. (2010) GABAergic control of neurite outgrowth and remodeling during development and adult neurogenesis: general rules and differences in diverse systems. *Front. Cell. Neurosci. 4*, 1−11.
(52) Gao, X. B., and van den Pol, A. N. (2000) GABA release from mouse axonal growth cones. *J. Physiol. (London, U.K.) 523*, 629−637.
(53) Lyck, R., Ruderisch, N., Moll, A. G., Steiner, O., Cohen, C. D., Engelhardt, B., Makrides, V., and Verrey, F. (2009) Culture-induced changes in blood-brain barrier transcriptome: implications for amino-acid transporters in vivo. *J. Cereb. Blood Flow Metab. 29*, 1491−1502.
(54) Ainla, A., Jansson, E. T., Stepanyants, N., Orwar, O., and Jesorka, A. (2010) A microfluidic pipette for single-cell pharmacology. *Anal. Chem. 82*, 4529−4536.
(55) Kress, H., Park, J. G., Mejean, C. O., Forster, J. D., Park, J., Walse, S. S., Zhang, Y., Wu, D. Q., Weiner, O. D., Fahmy, T. M., and Dufresne, E. R. (2009) Cell stimulation with optically manipulated microsources. *Nat. Methods 6*, 905−909.
(56) Gach, P. C., Wang, Y. L., Phillips, C., Sims, C. E., and Allbritton, N. L. (2011) Isolation and manipulation of living adherent cells by micromolded magnetic rafts. *Biomicrofluidics 5*, 1−12.

(57) Schoenherr, R. M., Ye, M. L., Vannatta, M., and Dovichi, N. J. (2007) CE-microreactor-CE-MS/MS for protein analysis. *Anal. Chem. 79*, 2230−2238.
(58) Kane, B. J., Zinner, M. J., Yarmush, M. L., and Toner, M. (2006) Liver-specific functional studies in a microfluidic array of primary mammalian hepatocytes. *Anal. Chem. 78*, 4291−4298.
(59) Huh, D., Hamilton, G. A., and Ingber, D. E. (2011) From 3D cell culture to organs-on-chips. *Trends Cell Biol. 21*, 745−754.
(60) Romanova, E. V., Fosser, K. A., Rubakhin, S. S., Nuzzo, R. G., and Sweedler, J. V. (2004) Engineering the morphology and electrophysiological parameters of cultured neurons by microfluidic surface patterning. *FASEB J. 18*, 1267−1269.
(61) Nemes, P., Marginean, I., and Vertes, A. (2007) Spraying mode effect on droplet formation and ion chemistry in electrosprays. *Anal. Chem. 79*, 3105−3116.
(62) Moini, M., Jones, B. L., Rogers, R. M., and Jiang, L. F. (1998) Sodium trifluoroacetate as a tune/calibration compound for positive- and negative-ion electrospray ionization mass spectrometry in the mass range of 100−4000 Da. *J. Am. Soc. Mass Spectrom. 9*, 977−980.